Published in final edited form as:

FASEB J. 2022 January ; 36(1): e22089. doi:10.1096/fj.202101270RR.

Antioxidant enzyme peroxiredoxin 5 regulates cyst growth and ciliogenesis via modulating Plk1 stability

Ewud Agborbesong[1,2,3], **Julie Xia Zhou**[1,2], **Linda Xiaoyan Li**[1,2], **James P. Calvet**[3], **Xiaogang Li**[1,2,#]

[1]Department of Internal Medicine, Mayo Clinic, Rochester, MN 55905.

[2]Department of Biochemistry and Molecular Biology, Mayo Clinic, Rochester, MN 55905

[3]Department of Biochemistry and Molecular Biology, University of Kansas Medical Center, Kansas City, KS 66160

Abstract

Oxidative stress is emerging as a contributing factor to the homeostasis in cystic diseases. However, the role of antioxidant enzymes plays in the pathogenesis of autosomal dominant polycystic kidney disease (ADPKD) remains elusive. Peroxiredoxin 5 (Prdx5) is an antioxidant enzyme that catalyzes the reduction of H_2O_2 and alkyl hydroperoxide and plays an important role in different biological processes. In this study, we show that Prdx5 is downregulated in a PKD mutant mouse model and ADPKD patient kidneys. Knockdown of Prdx5 resulted in the formation of cysts in a three-dimensional mouse IMCD cell Matrigel culture system. The mechanisms of Prdx5 deficiency mediated cyst growth include: 1) induction of oxidative stress as indicated by increased mRNA expression of heme oxygenase-1 (HO-1), an oxidant stress marker; 2) activation of Erk, S6 and mTORC1, which contribute to cystic renal epithelial cell proliferation and cyst growth; 3) abnormal centrosome amplification and multipolar spindle formation which result in genome instability; 4) upregulation of Polo-like kinase 1 (Plk1) and Aurora kinase A (AurA), important mitotic kinases involved in cell proliferation and ciliogenesis; 5) impaired formation of primary cilia in mouse IMCD3 and retinal pigment epithelial (RPE) cells, which could be rescued by inhibiting Plk1 activity; and 6) restraining the effect of Wnt3a and Wnt5a ligands on primary cilia in mouse IMCD3 cells, while regulating the activity of the canonical and non-canonical Wnt signaling in a separate cilia independent mechanism, respectively. Importantly, we found that targeting Plk1 with its inhibitor, volasertib, delayed cyst growth in *Pkd1* conditional knockout mouse kidneys. Together, these findings indicate that Prdx5 is an important antioxidant that regulates cyst growth via diverse mechanisms, in particular, the Prdx5-Plk1 axis, and that induction and activation of Prdx5, alone or together with inhibition of Plk1, represent a promising strategy for combatting ADPKD.

[#] To whom correspondence should be addressed. Xiaogang Li, Ph.D., Professor of Medicine, Department of Biochemistry and Molecular Biology and Medicine, Mayo Clinic, 200 1st Street, SW, Rochester, MN 55905, li.xiaogang@mayo.edu, Phone: 507-266-0110.

Author contributions: E.A. performed most experiments and data analysis. J.X.Z. and L.X.L. performed some of the experiments and data analysis. J.H. provided some antibodies and reagents. J.P.C. assisted in data analysis and manuscript preparation. X.L. supervised the whole project, data analysis and manuscript writing.

Disclosures: The authors declare no competing interests.

Introduction

Autosomal dominant polycystic kidney disease (ADPKD) is the most common inherited cystic renal disease which affects between 1 in 500 to 1 in 1,000 people [1]. Germline mutations in either the polycystic kidney disease 1 or 2 genes (PKD1 or PKD2), which encode polycystin-1 (PC1) and polycystin-2 (PC2), respectively, are the most common causes of ADPKD [2, 3]. This systemic disorder includes a variety of renal and extra-renal abnormalities that ultimately result in cystic and non-cystic features. The main clinical characteristic of the disease is the progressive increase in the number and size of renal cysts, with secondary destruction of renal parenchyma. Although the genetic basis of ADPKD is known, the molecular mechanisms underlying PKD phenotypes is still unclear, and safe and effective treatments are needed.

Though the pathogenesis of PKD remains poorly understood, various cellular defects have been suggested. For example, cyst development has been strongly associated with defects to the primary cilia, hence categorizing PKD as a ciliopathy [4, 5]. The primary cilium is a solitary, hair-like microtubule-based organelle anchored to the mother centriole and projects from the surface of almost all eukaryotic cells [6]. Primary cilia are involved in a wide range of sensory functions and are critical for developmental and physiological functions. Structural and functional cilia defects, including length abnormalities, have been characterized in several types of PKD. In addition, excessive reactive oxygen species (ROS) and oxidative stress are now recognized as a major contributing factor for polycystic kidney diseases [7, 8]. ROS which are normally produced in all types of cells, exert physiological and pathological effects if not eliminated by antioxidant enzymes [9, 10]. The expression of numerous protective antioxidant enzymes is reduced in cystic kidneys and contribute to ADPKD disease progression [11]. However, the role and mechanism of antioxidant enzymes in the regulation of cyst progression remain largely unknown.

The antioxidant enzyme peroxiredoxin 5 (Prdx5) is a member of the superfamily of six thiol-dependent peroxidases widely distributed among eukaryotes and prokaryotes. Prdx5 is ubiquitously expressed at high levels in different mammalian cells and normal tissues with a subcellular distribution in cytosol, mitochondria, peroxisomes, and the nucleus [12, 13]. Prdx5 functions mainly as a cytoprotector by reducing alkyl hydroperoxides and hydrogen peroxide (H_2O_2) during oxidative stress [14]. It exerts its antioxidant function by interacting with peroxisome-receptor-1 in different tissues under normal conditions and during inflammatory processes [15]. Prdx5 expression is frequently upregulated in different human cancers, including breast carcinoma [16], thyroid cancer [17], and in aggressive Hodgkin's lymphomas [18]. Prdx5 has also been upregulated in TNF-α or IL-1β treated cartilage explants from patients with osteoarthritis [19], resulting in the cartilage loss mediated by the disruption of Wnt/β-catenin pathway [20]. To the best of our knowledge, other than adrenocortical carcinoma [21], reduced levels of Prdx5 expression has not been reported in any other diseases.

In this study, we demonstrate the role and mechanisms of Prdx5 in the regulation of cyst growth and ciliogenesis. We show that the expression of Prdx5 is dramatically decreased in *Pkd1* mutant mouse renal epithelial cells and tissues as well as ADPKD patient

kidneys. Downregulation of Prdx5 results in cyst growth in mouse inner medullar collecting duct (IMCD) cell 3D-culture, induction of oxidative stress marker, HO-1, the activation of PKD associated signaling pathways, such as mTOR and Erk, genomic instability, and the upregulation of cell cycle regulators, such as Plk1 and Aurora A. Knockdown of Prdx5 also inhibits ciliogenesis in an AurA-Plk1 dependent manner. In addition, knockdown of Prdx5 restrains the effect of Wnt3a and Wnt5a ligands on cilia assembly and disassembly respectively and regulates canonical and non-canonical Wnt signaling in a ciliary independent manner. Furthermore, targeting Plk1 with its inhibitor, volasertib, delayed cyst growth in *Pkd1* conditional knockout mouse kidneys. Together, our results demonstrate that Prdx5 is important for renal development and its downregulation mediated upregulation of Plk1 may be sufficient to inhibit ciliogenesis and induce cyst growth in ADPKD kidneys. This is the first study to connect an antioxidant enzyme with cystogenesis and ciliogenesis, and induction and activation of Prdx5 alone, inhibition of Plk1 alone, or their combination, may represent a promising therapeutic strategy for ADPKD treatment.

Materials and Methods

Cell culture and reagents

Mouse inner-medullary collecting duct 3 (mIMCD3) cells and human retinal pigment epithelia (RPE) cells were maintained at 37 °C in 5% CO_2 in DMEM (Invitrogen) supplemented with 10% FBS. *Pkd1* WT and *Pkd1*-null MEK cells, derived from collecting ducts and sorted by the collecting duct marker Dolichos Biflorus Agglutinin (DBA) from kidneys of WT and *Pkd1*-null mice, were maintained as previously described [22, 23]. PH2 and PN24 cells (provided by S. Somlo through the George M. O'Brien Kidney Center, Yale University, New Haven, Connecticut, USA) were cultured as described previously [24].

The GIPZ Prdx5 short hairpin RNA (shRNA) and its vector GIPZ vector were purchased from Dharmacon. The PRDX5 (Myc-DDK-tagged) – Human peroxiredoxin 5 cDNA clone was purchased from OriGene.

Recombinant Mouse Wnt-3a ligand and Recombinant Human/Mouse Wnt-5a ligand were purchased from R&D Systems; were reconstituted in phosphate buffered saline (PBS) and kept at −20 °C. Wnt-3a ligand was used at a working concentration of 50ng/ml and Wnt-5a ligand was used at a concentration of 100ng/ml.

The proteasome inhibitor MG132 was purchased from Calbiochem (474790; San Diego, CA, USA). MG132 was dissolved in dimethyl sulfoxide (DMSO) at 10 mM as a stock solution and was kept at −20 °C.

The antibodies used for Western blot analysis included (a) anti-Prx5 (17724-I-AP) purchased from Proteintech; (b) anti-Aurora A/AIK (no. 3092S), anti-S6 (no. 2217), anti-ERK (no. 4696) and β-Catenin (Non-P)-S45 (no. 19807) purchased from Cell Signaling Technology; (c) the phosphorylated antibodies for ERK-T202/Y204 (no. 9101), S6-S235/236 (no. 2211) and mTOR1-S2448 (no. 5536) also purchased from Cell Signaling Technology; (d) anti-Plk1 (F-8, sc-17783) purchased from Santa Cruz Biotechnology Inc.; and (g) anti-actin antibody (A5316), and (h) anti-Flag M2 antibody (F1804) were

purchased from Sigma-Aldrich. The secondary antibodies, including donkey anti-rabbit IgG-horseradish peroxidase (sc-2313) and goat anti-mouse IgG-horseradish peroxidase (sc-2005) were purchased from Santa Cruz Biotechnology, Inc.

The antibodies used for Immunofluorescent staining included (a) anti-Prx5 antibody (17724-I-AP, 1:300), and anti-Flag tag (20543-I-AP, 1:200) were purchased from Proteintech; (b) anti-γ-tubulin antibody (GTU-88, 1:1000) and acetylated α-tubulin (6–11B-1, Sigma, T7451, 1:4000) purchased from Sigma Aldrich, (c) anti-Plk1 antibody (F-8, sc-17783, 1:200) and anti-α-tubulin antibody (DM1A, sc-32293, 1:1000) purchased from Santa Cruz Biotechnology Inc.; (d) anti- p-H3 (06–570, 1:500) was purchased from EMD Millipore; (f) Alexa Fluor secondary antibody 555 or 488 were purchased from Thermo Fisher; (g) Lotus Tetragonolobus Lectin (LTL) (FL-1321) and Dolichos Biflorus Agglutinin (DBA) (FL-1031) were purchased from Vector Laboratories.

Small interfering RNA (siRNA) transfection

The RNA oligonucleotides that specifically target mouse Prdx5 and human PRDX5 were purchased from Santa Cruz Biotechnology, Inc. The RNA oligonucleotides were transfected with Dharma-FECT siRNA transfection reagent (Dharmacon). 24 h or 48 h after transfection, cells were harvested for further analysis.

Generation of stable Prdx5 knockdown IMCD3 cell line

HEK293T cells were co-transfected with lentiviral plasmid carrying Prdx5 shRNA or control empty vector pGIPZ-NS, psPAX2 packaging plasmid, and pMD2.G envelope plasmid, using calcium phosphate. Twelve hours later, medium containing the transfection reagent was removed and replaced with fresh complete DMEM plus 10% FBS and penicillin/streptomycin. Forty-eight hours later, cultures containing lentiviral particles were harvested from HEK293T cells. IMCD3 cells were then infected with appropriate amounts of lentiviral particles together with 5 μg/ml polybrene (Sigma, St Louis, MO). Twenty-four hours later, virus-containing medium was removed and replaced with fresh medium plus 10 μg/ml puromycin. Two days after selection, all the cells were GFP positive, which indicated the very high efficiency of transduction. Subsequently, several clones were selected for and cultured in medium with 10 μg/ml puromycin to be used for Western blot analysis, immunostaining analysis and 3D Matrigel cultures.

Plasmid transfection

PN24 cells were seeded on coverslips in 6-well dishes to about 50–70% confluency at the time of transfection. For rescue experiments, 3 μg Myc-Flag-PRDX5 and 5 μl lipofectamine 3000 were mixed in 250 μl serum- and antibiotic-free DME-F/12 and incubated for 15 min at room temperature. New DME-F/12 medium was added to the cells prior to transfer of the transfection reagent, which was gently dripped onto the cells and swirled to make sure it was dispersed well. After cells were incubated with transfection medium for 6 hr, the medium was replaced with serum-containing DME-F/12 medium for 24 hr, and then serum deprived for 48 hours to induce ciliogenesis.

RNA extraction and quantitative reverse transcription-polymerase chain reaction (qRT-PCR)

Total RNA was extracted using the RNeasy Plus Mini Kit (QIAGEN). Total RNA (1 μg) was used for RT reactions in a 20 μl reaction to synthesize cDNA using an iScript cDNA Synthesis Kit (Bio-Rad). RNA expression profiles were analyzed by real-time PCR using iTaq SYBR Green Supermix with ROX (Bio-Rad) in an iCycler iQ Real-Time PCR Detection System. The complete reactions were subjected to the following program of thermal cycling: 40 cycles of 10 s at 95 °C and 20 s at 60°C. A melting curve was run after the PCR cycles followed by a cooling step. Each sample was run in triplicate in each experiment, and each experiment was repeated 3 times. Expression levels of target genes were normalized to the expression level of actin and GAPDH.

Protein extraction and Western blot analysis

Cell pellets were collected and resuspended in lysis buffer (20 mM Tris-HCl, pH 7.4, 150 mM NaCl, 10% glycerol, 1% Triton X-100, 1 mM Na3VO4, 25 mM β-glycerolphosphate, 0.1 mM PMSF, Roche complete protease inhibitor set, and Sigma-Aldrich phosphatase inhibitor set). The resuspended cell pellet was incubated on ice for 30 min with intermittent vortexing every 10 min for 20s and then centrifuged at 20,000 g for 30 min. The supernatants were collected for Western blot analysis.

Flow cytometry analysis

Flow cytometry analysis was performed as described. Prdx5 stable knockdown IMCD3 cells were synchronized by serum starvation for 24 h, then exposed to normal growth culture medium containing 10% FBS. 48h after normal growth conditions, the cells were collected by trypsinization and washed twice with PBS, fixed with cold 75% ethanol, and stored at −20°C overnight. Fixed cells were washed once with cold PBS and centrifuged for 5 min at 4000 rpm to remove ethanol. The supernatant was aspirated, and the cell pellets were resuspended in 100μl of PBS. 300μl of PBS containing Triton-X (0.3%), propidium iodide (PI) (0.05 mg/ml) and RNAse A (0.3 mg/ml) was added to cell suspension and incubated at room temperature for 15 min, and then subjected to flow cytometry analysis. The cell suspension was analyzed on a FACSCanto flow cytometer (BD Biosciences). Analysis was carried out using FlowJo software 10.7.

Tissue immunofluorescence staining

Paraffin-embedded sections (5 μm) were subjected to staining. After antigen retrieval, tissue sections were incubated overnight with a polyclonal rabbit anti-Prx5 primary antibody (Proteintech; 17724-I-AP, 1:300 dilution) and an Alexa Fluor 488–conjugated donkey anti-rabbit immunoglobulin G (IgG) (H+L) secondary antibody (Thermo Fisher Scientific, 1:1000), and LTL, or DBA. Kidney sections were counterstained by 4′,6-diamidino-2-phenylindole (DAPI). Images were analyzed using a Nikon Eclipse 80i microscope.

Cell immunofluorescence analysis

Cells grown on coverslips were rinsed with 1x phosphate-buffered saline (PBS), fixed in cold methanol for 10 min at −20°C, followed by permeabilization with 0.2% Triton X-100

for 15 min at 37°C, or cells were fixed with 4% paraformaldehyde (PFA) for 10 min at 37°C, followed by permeabilization with 0.2% Triton X-100 at room temperature for 10 min. Cells were then washed by PBS three times, and blocked in 2% BSA and sequentially incubated with primary and secondary antibodies.

3D spheroid model for mIMCD3 cells

Prdx5 stable knockdown mouse IMCD3 cells were seeded in Matrigel 20. In brief, mIMCD3 stable knockdown cells were treated with trypsin for 3–5 min and resuspended in prewarmed (37 °C) medium containing 20nM volasertib, in a concentration of 100,000 cells per milliliter. Next, 100 μl of cell suspension was gently mixed with 100 μl of growth factor depleted Matrigel (BD Biosciences) in a 1.5 ml microcentrifuge tube. Then the cell-Matrigel mixture was transferred to each well of a 24 well plate. After polymerization for 30 min at 37 °C, just enough warmed complete culture medium was added to cover the matrix. The cells were cultured at 37 °C with 5% CO2. In general, the cells formed spheroids with cleared lumens in 2 to 3 days.

Human samples

De-identified human ADPKD and normal human kidney (fresh frozen and formalin-fixed, paraffin-embedded sections) were obtained from the Mayo Translational Polycystic Kidney Disease Center. Informed consent was obtained.

Mouse strains and treatment

Pkd1$^{fl/fl}$*:Pkhd1-Cre* mice were generated by cross-breeding *Pkd1*$^{fl/+}$*:Pkhd1-Cre* female mice with *Pkd1*$^{fl/+}$*:Pkhd1-Cre* male mice. The kidneys were harvested and analyzed at postnatal day 21. Littermate controls were used in all animal experiments. *Pkd1*$^{fl/fl}$*:Pkhd1-Cre* pups were injected i.p. with volasertib (5 mg/kg, dissolved in DMSO, with a final DMSO concentration of 10% [v/v] in PBS) or DMSO (control) daily from P8 to P19, and kidneys were harvested and analyzed at P20.

Measurement of cyst area.

The cyst volume was quantified in whole kidney after H&E staining using Image-Pro Plus v5 software (Media Cybernetics). The cyst area was calculated as (cyst area/total area) × 100%. Two sections from both kidneys were analyzed for each mouse.

Quantitative BUN determination.

Serum samples were first diluted 5-fold in distilled water prior to assay. Next, 5 μl water (blank), 5 μl standard (50 mg/dl), and 5 μl samples were transferred in triplicate into wells of a clear-bottom 96-well plate. 200 μl of working reagent was added and tapped lightly to mix, and the samples were incubated 20 minutes at room temperature. Optical density was read at 520 nm.

Statistical analysis

All data are presented as the mean ± SD. Cilia length and cyst diameter were measured using ImageJ NIH software. All statistical analyses were performed using either SPSS

Statistics 22 software or GraphPad Prism, version 9.1.0. *P* values were calculated by two-tailed unpaired Student's *t* test or one-way analysis of variance (ANOVA), and $P < 0.05$ were considered statistically significant.

Results

The expression of Prdx5 is downregulated in *Pkd1* mutant renal epithelial tissues and ADPKD tissues.

To determine the involvement of peroxiredoxins (Prdxs) in ADPKD, we analyzed the expression pattern of Prdx isotypes (Prdx1, Prdx2, Prdx3, Prdx4, Prdx5, and Prdx6) in *Pkd1* mutant renal epithelial cells by quantitative real-time polymerase chain reaction (qRT-PCR). We found that the expression of Prdx1 and Prdx2 was downregulated in *Pkd1* null (NULL) mouse embryonic kidney (MEK) cells compared to *Pkd1* wild type (WT) MEK cells, whereas their expression was not changed in the postnatal *Pkd1* homozygous PN24 cells compared to *Pkd1* heterozygous PH2 cells (Supplemental Figure 1A – 1D). The expression of Prdx4 showed no difference between WT and NULL MEK cells and was undetected in PH2 and PN24 cells (Supplemental Figure 1E). The expression of Prdx6 showed no difference between WT and NULL MEK cells nor between PH2 and PN24 cells (Supplemental Figure 1F and 1G). The expression of Prdx3 (Supplemental Figure 1H and 1I) and Prdx5 (Figure 1A) was decreased both in NULL MEK and PN24 cells compared to WT and PH2 cells. We further found that the expression of Prdx3 was upregulated (Supplemental Figure 1J), and the expression of Prdx5 was downregulated (Figure 1B) in postnatal day 21 (P21) kidneys from *Pkd1*$^{fl/fl}$*:Pkhd1-Cre* mice, a well-characterized animal model for ADPKD, compared to that in kidneys from age-matched wild type mice. These results guided us to investigate the role of Prdx5 in ADPKD.

We further found that the expression of Prdx5 protein was also downregulated in *Pkd1* NULL MEK and PN24 cells (Figure 1C) and in P21 kidneys from *Pkd1*$^{fl/fl}$*:Pkhd1-Cre* mice compared to controls as examined by Western blot analysis (Figure 1D). The expression of PRDX5 mRNA and protein were also decreased in human ADPKD kidneys compared with normal human kidneys (NHK) as examined by qRT-PCR and Western blot (Figure 1E and 1F). Our immunofluorescent analysis further indicated that Prdx5 was mildly co-localized with lotus tetragonolobus lectin (LTL), a proximal tubule marker, in wild type and *Pkd1* mutant mouse kidneys (Figure 1G, *right panel*), and in human ADPKD kidneys (Figure 1H, *right panel*). In addition, Prdx5 co-localized with dolichos biflorus agglutinin (DBA), a collecting duct marker, in wild type mouse kidneys (Figure 1G, *left panel*) and normal human kidneys (Figure 1H, *left panel*) but not in *Pkd1* mutant mouse kidneys and human ADPKD kidneys, suggesting that the absence of Prdx5 in cyst lining epithelial cells might contribute to cyst growth in ADPKD.

Knockdown of Prdx5 promotes cyst growth in mouse IMCD3 cell 3D culture.

To determine the role of Prdx5 in the regulation of cyst growth, we stably knocked down Prdx5 with shRNA in mouse inner medullary collecting duct 3 (IMCD3) cells. The knockdown efficiency of Prdx5 was confirmed by Western blot and qRT-PCR analysis (Supplemental Figure 2A and 2B). By culturing Prdx5 stable knockdown IMCD3 cells and

vector control transfected cells in three-dimensional (3D) Matrigel-collagen I gels, we found that knockdown of Prdx5 increased the formation of cyst-like cell clusters with discernible lumens compared to those in the control vector 3D cultures (Figure 2A and Supplemental Figure 2C). Knockdown of Prdx5 significantly increased the diameters of cysts formed in 3D cultures at day 7 compared to those in control shRNA 3D cultures at day 7 (Figure 2B). Previous studies suggest that cystic kidneys have altered redox metabolism which may result in a state of chronic oxidative stress. To determine whether the downregulation of Prdx5 contributes to oxidative stress in PKD, we assessed the expression of HO-1, a widely accepted marker of oxidative stress in Prdx5 siRNA depleted *Pkd1* homozygous PN24 cells. We found that knockdown of Prdx5 increased the mRNA level of HO-1 compared to control siRNA treated cells (Figure 2C). In addition, knockdown of Prdx5 increased the accumulation of lipid droplets as examined by BODIPY staining [25], a measurement that is generally used to monitor oxidative stress mediated lipid ROS in cell membranes (Supplemental Figure 2D). These results suggest that downregulation of Prdx5 contributes to oxidant stress and cyst growth in *Pkd1* mutant kidneys.

Knockdown of Prdx5 activates PKD associated signaling pathways in renal epithelial cells.

To investigate the mechanism(s) by which downregulation of Prdx5 promotes cyst growth, we examined the signaling pathways known to be associated with cystic renal epithelial cell proliferation and stress response, such as the mitogen-activated protein kinase (MAPK) and the mammalian TOR (mTOR) [26, 27]. We found that knockdown of Prdx5 increased the phosphorylation of ERK (p-ERK) and mTOR (p-mTOR) in mouse IMCD3 cells (Figure 2D, Supplemental Figure 3A and 3B). In addition, we found that knockdown of Prdx5 increased the phosphorylation of ERK and S6 in *Pkd1* homozygous PN24 cells (Figure 2E). These results suggest that downregulation of Prdx5 promotes cyst growth possibly through activation of MAPK and mTOR signaling pathways.

Knockdown of Prdx5 leads to centrosome amplification and multipolar spindle formation in IMCD3 cells.

To further gain insights into how downregulation of Prdx5 regulates renal epithelial cell proliferation and cyst formation, we determined whether knockdown of Prdx5 affects cell cycle by flow cytometry analysis in Prdx5 stable knockdown IMCD3 cells. We found that stable knockdown of Prdx5 resulted in an increased percentage of cells in the S-phase compared to control cells (Supplemental Figure 3C and 3D). Furthermore, knockdown of Prdx5 resulted in a decreased percentage of cells in the G2/M-phase, which was further confirmed by immunofluorescent staining with phosphorylated histone H3 (p-H3), a cell cycle marker for the late G2/M phases (Supplemental Figure 3E and 3F). Centrosome duplication and maturation occur during the S-phase and G2-phase, respectively [28]. We found that knockdown of Prdx5 resulted in abnormal centrosome amplification (≥3 centrosomes per cell) (Figure 3A and 3B) and spindle multi-polarity in mouse IMCD3 cells (Figure 3C and 3D). In mammalian cells, the mitotic protein kinases Polo-like kinases (Plks) play essential roles in cell division and checkpoint regulation of mitosis. Plk1 has been emerging as a regulator of centriole duplication and its overexpression leads to centrosome aberrations [29]. Similarly, Aurora A kinase (AurA), another mitotic kinase, has also been reported to regulate centrosome duplication, with its elevated levels resulting

in abnormal centrosome amplification [30]. We found that knockdown of Prdx5 resulted in the upregulation of Plk1 and AurA proteins as examined by Western blot (Figure 3E), whereas there was no change of their mRNAs (Figure 3F). These results suggest that the stability of Plk1 and AurA proteins may contribute to Prdx5 deficiency-induced centrosome amplification.

Prdx5 knockdown decreases the number of ciliated cells and cilia length in mouse IMCD3 and retinal pigment epithelial (RPE) cells.

Defects in primary cilia formation and cilia-mediated signaling activity are also key factors that lead to cyst formation [22, 31, 32]. Because Plk1 and AurA are components of the cilia assembly/disassembly machinery [33, 34], which are increased in Prdx5 knockdown mIMCD3 cells (Figure 3E), we hypothesized that Prdx5 may be involved in the regulation of ciliogenesis. We indeed found that stable knockdown of Prdx5 resulted in the decreased percentage of ciliated cells and cilia length in mouse IMCD3 cells stained with acetylated α-tubulin (Ac-α-tub) compared to the control shRNA transfected cells after 48 h serum-starvation (Figure 4A – 4C). We further found that knockdown of Prdx5 with small interfering RNA (siRNA) also decreased the percentage of ciliated cells and cilia length in retinal pigment epithelial (RPE) cells (Figure 4D – 4F). The knockdown efficiency with PRDX5 siRNA in RPE cells was confirmed by Western blot and qRT-PCR analysis (Supplemental Figure 4A and 4B). In addition, we found that PLK1 and AURA protein levels were upregulated in PRDX5 knockdown hTERT-RPE cells compared to control cells (Supplemental Figure 4C). These results support that Prdx5 is involved in primary cilia biogenesis.

Knockdown of Prdx5 inhibits ciliogenesis by activating Plk1

Both Plk1 and AurA are located at the basal body, a ciliary structure that differentiates from the mother centriole in quiescent cells, to regulate cilia assembly/disassembly [33, 34]. We hypothesized that Prdx5 might regulate ciliogenesis through affecting the basal body localization of Plk1 and AurA in quiescent cells. Following serum starvation for 24 hours, we found that knockdown of Prdx5 increased the percentage of cells with Plk1 at the basal bodies in mouse IMCD3 cells compared to that in control shRNA transfected cells (Figure 5A and 5B). Likewise, knockdown of PRDX5 also increased the percentage of cells with PLK1 (Supplemental Figure 4D and 4E) and AURA (Supplemental Figure 4F and 4G) at the basal bodies in RPE cells compared to control siRNA transfected cells. The increase of Plk1 and AurA at the basal bodies in Prdx5 knockdown cells suggests that Prdx5 may regulate ciliogenesis through Plk1 and AurA. To test this hypothesis, we treated Prdx5 knockdown cells with the Plk1 inhibitor volasertib [35]. We found that inhibition of Plk1 with volasertib rescued the percentage of ciliated cells, as well as increased cilia length in Prdx5 knockdown IMCD3 cells after 24 hours serum starvation, compared with control cells (Figure 5C – 5E). These results suggest that knockdown of Prdx5 possibly mediates ciliogenesis defects by affecting the localization and activity of Plk1, and the AurA-Plk1 cilia disassembly axis.

Exogenous expression of Prdx5 rescues ciliogenesis in renal epithelial cells.

To further evaluate the role of Prdx5 on ciliogenesis, we performed a rescue experiment. We transfected Myc and flag tagged PRDX5 (Myc-Flag-PRDX5) into Prdx5 stable knockdown

mouse IMCD3 cells followed by serum starvation. We found that ectopic expression of Prdx5 increased the cilia length in Prdx5 depleted mouse IMCD3 cells comparable to that in vector transfected Prdx5 depleted cells (Supplemental Figure 5A and 5B). In addition, we found that ectopic expression of Prdx5 decreased the phosphorylation of Erk, and mTOR (Supplemental Figure 5C). In addition, we found that ectopic expression of Prdx5 increased cilia length in Prdx5 upregulated *Pkd1* mutant PN24 cells comparable to that in vector transfected cells (Supplemental Figure 5D and 5E). Ectopic expression of Prdx5 resulted in the decrease of the phosphorylation of Erk, and S6 (Supplemental Figure 5F). These results suggest that overexpression of Prdx5 could rescue ciliogenesis defects in Pkdx5 depleted cells and *Pkd1* mutant renal epithelial cells and Prdx5 might also be involved in ERK and mTOR signaling pathway mediated cell proliferation.

Inhibition of Plk1 reduces cyst growth in 3D cultures and in *Pkd1* mutant kidneys.

Dysregulation of ciliogenesis has been proposed to enhance cyst growth in ADPKD [36]. Furthermore, Plk1 activity has been implicated in cyst growth in polycystic kidney disease [37]. Since inhibition of Plk1 rescued the defects of ciliogenesis in Prdx5 knockdown cells, we hypothesized that treatment with Plk1 inhibitor would delay cyst growth in Prdx5 stable knockdown IMCD3 cell 3D cultures. To test this hypothesis, we seeded Prdx5 stable knockdown IMCD3 cells in Matrigel in a 1:1 ratio with the culture medium containing 20nM volasertib, and cysts were observed as demonstrated by the scheme in Figure 6A. We found that inhibition of Plk1 decreased cyst growth characterized by the decrease of cyst diameters in Prdx5 knockdown IMCD cell 3D cultures but did not affect cyst growth in 3D culture with control cells (Figure 6B and 6C). These results suggest that Prdx5 may act through Plk1 to negatively regulate cyst development.

Importantly, we found that the protein levels of Plk1 were upregulated in both $Pkd1^{fl/fl}$ mouse kidneys and human ADPKD kidneys compared to those in wild type mouse kidneys and normal human kidneys (Figure 6D). To investigate whether inhibition of Plk1 delayed cyst growth *in vivo*, we treated $Pkd1^{fl/fl}$*:Pkhd1:Cre* mice with Plk1 inhibitor [35]. We found that administration of volasertib (5 mg/kg) (n = 5) delayed cyst growth, as indicated by decreased cyst index, kidney weight to body weight (KW/BW) ratios and blood urea nitrogen (BUN) levels (Figure 6E – 6H) in postnatal day 20 (PN20) $Pkd1^{fl/fl}$*:Pkhd1-Cre* mice compared to those in age-matched DMSO-injected $Pkd1^{fl/fl}$*:Pkhd1-Cre* mice (n = 5). In addition, treatment with volasertib did not affect the body weight of both the treated and control groups (Figure 6I). These results suggest that targeting Plk1 by pharmacological inhibition might be a novel therapeutic strategy for ADPKD treatment.

Plk1 regulates the transcription of Prdx5

Inhibition of Plk1 in Prdx5 knockdown cells was found to play a considerable role in rescuing ciliogenesis and cystogenesis defects. As such, we wanted to gain more insights into the relationship between Prdx5 and Plk1. As previously examined, knockdown of Prdx5 resulted in the upregulation of Plk1 protein level (Figure 3E and Supplemental Figure 4C), however, did not affect the mRNA level of Plk1 as measured by qRT-PCR (Figure 3F and Supplemental Figure 6A), suggesting that Prdx5 knockdown might affect Plk1 protein stability. To support this hypothesis, we found that treatment with MG132

(10 μM), a proteasome inhibitor, increased Plk1 protein level in Prdx5 knockdown cells compared to that in control shRNA transfected cells treated with MG132 (Supplemental Figure 6B). These results suggest that knockdown of Prdx5 increases Plk1 protein stability by interfering with the ubiquitin-proteasome protein degradation pathway. Given that Plk1 has been reported to regulate gene transcription, we investigated whether Plk1 plays a role in the regulation of Prdx5. We found that treatment with Plk1 inhibitor volasertib increased the mRNA and protein levels of Prdx5 (Supplemental Figure 6C and 6D) in both mouse IMCD3 and RPE cells, respectively. Put together, these results suggest that Plk1 may play a role in the transcription regulation of Prdx5, and there exists a negative feedback loop between Prdx5 and Plk1 proteins.

Loss of Prdx5 regulates Wnt signaling in a cilia dependent and independent manner in IMCD3 cells.

Canonical and noncanonical Wnt signaling has been associated with cyst formation and progression in ADPKD animal models and patients [38–40]. Primary cilia play a role in the activation of both canonical and noncanonical Wnt signaling pathways, and Wnt signaling also regulates ciliogenesis [41], both of which may contribute to renal cystic disease by disrupting Ca^{2+} signaling and/or planar cell polarity (PCP) processes in renal epithelial cells [42]. To test whether knockdown of Prdx5 mediated ciliogenesis defects affect Wnt signaling pathway, first, we analysed the expression of Wnt ligand genes in Prdx5 knockdown cells by qRT-PCR analysis. We found that knockdown of Prdx5 decreased the expression of canonical Wnt ligands, including Wnt3a and Wnt8a (Figure 7A and 7B), and non-canonical Wnt ligands, including Wnt5a and Wnt10a (Figure 7C and 7D) in mouse IMCD3 cells compared to control cells. Activation of the canonical Wnt pathway leads to stabilization of β-catenin. To verify the effect of Prdx5 knockdown on canonical Wnt activity, we examined the expression of active β-catenin. We found that knockdown of Prdx5 decreased the protein level of active β-catenin (Supplemental Figure 7A) compared to control mouse IMCD3 cells. This suggests that knockdown of Prdx5 inactivates canonical Wnt signaling and inhibits non-canonical Wnt signaling pathway. To gain insights into the possible involvement of cilia in the regulation of Wnt signaling in the Prdx5 knockdown cells, we tested the responses of Prdx5 knockdown cells to Wnt3a (canonical Wnt ligand) and Wnt5a (non-canonical Wnt ligand), reported to regulate cilia assembly and disassembly, respectively [33, 43]. Prdx5 stable knockdown and control IMCD3 cells were serum-starved and stimulated with Wnt3a and Wnt5a ligands according to the experimental schedule illustrated in Figure 7E. To ensure the efficacy of the ligand treatment, cells were harvested and the gene expression of Wnt3a and Wnt5a were examined by qRT-PCR (Figure 7F). We found that stimulation with Wnt3a increased the percentage of ciliated cells and cilia length in control cells as reported in literature [43] but did not affect ciliogenesis in Prdx5 knockdown IMCD3 cells (Figure 7G – 7I). In contrast, stimulation with Wnt5a decreased the percentage of ciliated cells and cilia length in control cells as reported in literature [33] but did not affect ciliogenesis in Prdx5 knockdown cells (Figure 7J – 7L). These results suggest that loss of Prdx5 decreases the responsiveness of renal epithelial cells to Wnt3a and Wnt5a mediated ciliogenesis. In addition, we found that knockdown of Prdx5 decreased the expression of canonical Wnt target gene Axin2 and non-canonical Wnt signaling target gene protein tyrosine kinase 7 (Ptk7). However, stimulation with Wnt3a resulted in the

upregulation of Axin2 (Supplemental Figure 7B) and active β-Catenin (active) in Prdx5 knockdown cells (Supplemental Figure 7C), suggesting activation of the canonical Wnt signaling pathway. Furthermore, stimulation with Wnt5a had no effect on the expression of Ptk7 in Prdx5 knockdown cells (Supplemental Figure 7D). These results suggest that loss of Prdx5 regulates the Wnt3a mediated canonical Wnt signaling pathway in a cilia independent manner and Wnt5a mediated non-canonical Wnt signaling pathway in a cilia dependent manner. Moreover, downregulation of the non-canonical Wnt signaling in Prdx5 deficient cells may be a potential mechanism for cyst growth in ADPKD.

Discussion

Previous study suggests that the expression of numerous protective antioxidant enzymes is reduced in cystic kidneys and contributes to PKD disease progression. However, the mechanisms that underlie the role of antioxidant enzymes in cyst growth in ADPKD remain unclear. Peroxiredoxins are a family of antioxidant enzymes with six members (Prdx1 to Prdx6) that catalyzes the reduction of hydrogen peroxide and exerts protective antioxidant role in mammalian cells. All Prdxs are expressed in different cell types in the kidney. With the comparison of the mRNAs of the six Prdxs in *Pkd1* mutant renal epithelial cells and tissues, we found that only the expression of Prdx5 mRNA remained unfluctuating, whereas the expression of mRNAs of Prdxs 1, 2, 3, 4 and 6 varied at different stages of the disease (Supplemental Figure 1). This suggested that Prdx5 should play a more consistent role than other Prdxs in ADPKD. In this study, we further show that the antioxidant enzyme, Prdx5, is downregulated in *Pkd1* mutant renal epithelial cells and tissues as well as in human ADPKD kidneys. We further show that knockdown of Prdx5 results in cyst formation in mouse IMCD3 cell 3D cultures. To understand the underlying mechanisms, we show that knockdown of Prdx5: 1) induces the expression of HO-1, indicative of increased oxidative stress; 2) increases the activation of Erk, S6 and mTOR which have been associated with cystic renal epithelial cell proliferation; 3) increases centrosome amplification and multipolar spindle formation which may result in genome instability in ADPKD; 4) increases the expression of Plk1 and AurA, two cell cycle checkpoint kinases reported to regulate cell proliferation and other cellular signaling; and 5) inhibits ciliogenesis, possibly by increasing the basal body localization AurA and Plk1 and the activity of AurA-Plk1 cilia axis (Figure 8). Importantly, we showed that treatment with a Plk1 specific inhibitor, volasertib, delayed cyst growth in *Pkd1* knockout mouse kidneys. We also show that knockdown of Prdx5 resulted in the downregulation of both canonical and non-canonical Wnt ligands and Wnt target genes. However, stimulation with Wnt3a resulted in the upregulation of canonical Wnt targets, whereas stimulation with Wnt5a had no effect on non-canonical Wnt targets in Prdx5 knockdown cells, suggesting that Prdx5 regulates canonical Wnt signaling in a cilia independent mechanism. This study suggests that downregulation of the antioxidant enzyme Prdx5 may contribute to ADPKD pathogenesis by affecting oxidative stress, cell proliferation, genome instability, ciliogenesis and Wnt signaling, and is the first study for the mechanistic understanding of how antioxidant enzymes regulate cyst growth in the context of ADPKD disease.

The protective role of antioxidants in the pathogenesis of PKD has been reported in mouse and rat PKD models. Pharmacological reduction of renal antioxidant protection exacerbates

PKD [44] while pharmacological induction of antioxidant enzymes represents a promising strategy for the protection of kidney tissue from oxidative injury and for the treatment of ADPKD [45]. In addition, the presence of increased genomic instability in ADPKD [42] may contribute to the genetic diversity of ADPKD cystic cells and possibly trigger cystogenesis [46]. However, the mechanisms that result in genome instability in ADPKD are not fully understood. Thus far, it is reported that the loss of polycystin-1 (PC-1) disrupts the maintenance of centrosome integrity which subsequently leads to genomic instability, resulting in an increase of cell proliferation. We noted an increase in genomic instability as indicated by the increased centrosome amplification and multi-polar spindle formation in Prdx5 knockdown cells. The presence of centrosome and cytokinesis defects in Prdx5 knockdown cells correlated with the increased expression of the mitotic kinases Plk1 and Aurora A, known to regulate spindle pole alignment, centrosome duplication and centrosome maturation. Overexpression of Plk1 and AurA are reported to result in the increased percentage of cells with abnormal centrosome amplification. Our results suggest that the downregulation of Prdx5 contributes to cyst growth and disease progression in ADPKD by modulating genomic instability.

Prdx5 has been reported to function as a cytoprotector in several diseases. For example, studies indicated Prdx5 functions as a protective regulator in fatty liver disease in Prdx5 knockout mice (8-week-old), suggesting a role of Prdx5 in obesity-related metabolic diseases [47]. It has also been reported that knockout of Prdx5 results in the development of malignant cancers, mainly lymphoma, in mice older than 14 months, suggesting a role of Prdx5 as a tumor suppressor [48]. However, the renal phenotype might have been overlooked in these reports. In this study, we show that knockdown of Prdx5 resulted in the formation of cyst growth in 3D cultures. Whether deletion of Prdx5 results in renal cyst in Prdx5 knockout mice is hard to predict. In ADPKD, renal cyst formation and progression requires the cooperation of multiple mechanisms, which is supported by the fact that targeting one signaling pathway only delays cyst growth but cannot cure PKD. With the multiple factors associated with ADPKD cyst progression observed in Prdx5 knockdown cells, it is possible that Prdx5 requires the PKD gene mutation to enhance its role in cyst formation in kidneys and thereby enhance disease progression.

There is increasing evidence to suggest that oxidative stress and the generation of reactive oxidative species (ROS) is increased in ADPKD patients. Oxidative stress is reported to regulate the activation of signaling pathways associated with cell proliferation including MAPK signaling and mTOR signaling pathways [49]. AurA is also reported to regulate multiple molecules involved in cell proliferation and signaling pathways, such as MEK/ERK and mTOR signaling pathways [50], which is upregulated in Prdx5 knockdown cells. We therefore hypothesized that the MAPK and mTOR signaling pathways would be affected. This idea was supported by the increased expression of phosphorylated Erk and mTORC1, commonly attributed to cystic kidneys, suggesting that the downregulation of Prdx5 may contribute to cyst growth in ADPKD by modulating cell proliferation through the MAPK and mTOR signaling pathways. Oxidative stress and ROS have also been associated with fatty acid or lipid peroxidation [51]. Metabolic reprogramming has recently been associated with ADPKD disease and several studies have reported that fatty acid oxidation (FAO) is impaired in ADPKD [52]. Furthermore, lipid peroxidation is upregulated in *Pkd1* mutant

renal epithelial cells as detected by BODIPY staining and 4-hydroxynonenal (4-HNE), a secondary product and marker of lipid oxidation [53]. In this study, we found that depletion of Prdx5 resulted in the upregulation of HO-1 suggesting increased oxidative stress. We also found that depletion of Prdx5 affected lipid peroxidation indicated by the formation of lipid droplets by BODIPY staining, suggesting that the downregulated Prdx5 might contribute to the impaired fatty acid oxidation observed in ADPKD kidneys, which should be further investigated.

Structural and functional defects of the primary cilia have been reported to cause cystic diseases. However, the implications of cilia length in cystic kidney disease pathogenesis remains unclear. Thus far, reports of cilia length and its relevance in ADPKD remain controversial. Some studies report that recovering cilia length would ameliorate disease progression, while others report that the complete removal of cilia improves disease progression [54]. Plk1 is a key cell cycle regulator associated with cilia disassembly [34, 37]. Furthermore, Plk1 is an important oncogene whose overexpression serves as an important marker for cancer prognosis [55]. Plk1 was upregulated in Prdx5 knockdown IMCD3 cells, which correlated with the formation of short cilia and cyst growth in 3D cultures. Inhibition of Plk1 rescued the cilia defect in Prdx5 knockdown mouse IMCD3 cells. Inhibition of Plk1 also decreased cyst diameter in Prdx5 knockdown cells yet had no effect on control cells. These results suggest that Prdx5 through Plk1, may regulate cilia disassembly machinery and cyst growth. Studies have revealed that targeting PLK1 may be a novel approach for overcoming drug resistance in cancer chemotherapy [56, 57]. So far, very little is known about Polo-like kinase inhibitors as therapeutic agents in ADPKD or kidney diseases. We found that pharmacologically targeting Plk1 delayed cyst growth in *Pkd1* mutant mouse kidneys, supporting a novel Prdx5-Plk1 axis, in regulating cilia disassembly and cyst growth in ADPKD. As such, the induction of Prdx5 together with the inhibition of Plk1 may serve as a potential therapeutic strategy for the treatment of ADPKD and ciliopathies. Our results also suggest that it is indeed possible that cilia are shorter in PKD cystic kidneys compared to wild type controls and that the recovery of cilia length delays cyst growth and ameliorates disease progression. However, we cannot exclude a possibility that prolonged exposure to oxidative stress present in the cystic environment may affect the cilia over time, since there is evidence to suggest that different levels of oxidative stress may vary the length of primary cilia [58]. For the future, it would be interesting to determine whether exposing Prdx5 knockdown cells to varying degrees of oxidative stress would affect cilia length, and how this would affect cyst growth and cilia associated cell signaling pathways. This may shed some light on the controversy of cilia length and its implication in PKD disease severity.

Prdx5 is constitutively expressed at high levels in different mammalian cell lines and normal tissues, however, the specific transcription factors involved in the regulation of its expression have not been completely identified. A study reports that c-Myc directly modulates PRDX5 expression by interacting with putative responsive elements in the 5′-flanking regions of the gene to positively regulate the expression of Prdx5 [59]. It has been reported that c-Myc is upregulated in ADPKD kidneys [60], which should increase the expression of Prdx5. However, we found that Prdx5 was downregulated in ADPKD, suggesting that Prdx5 is not regulated by c-Myc in *Pkd1* mutant renal epithelial cells and tissues. Interestingly, we found

that inhibition of Plk1 in mouse IMCD3 and RPE cells resulted in the upregulation of Prdx5, suggesting that Plk1 may be a novel regulator of Prdx5 and Plk1 and Prdx5 may form a negative feedback loop in ADPKD kidneys.

Primary cilia are reported to play a role in the regulation of both canonical and non-canonical Wnt signaling pathways. Whilst it is well accepted that normal ciliogenesis is essential for non-canonical Wnt signaling pathway (planar cell polarity, PCP), it's role in canonical Wnt signal transduction activation remains controversial. We found that knockdown of Prdx5 resulted in the downregulation of the canonical Wnt signaling pathway and non-canonical Wnt pathway as indicated by the downregulation of the downstream target genes Axin2 and Ptk7 respectively. Stimulation of cells with Wnt3a ligand is reported to enhance cilia assembly, while stimulation with Wnt5a enhances cilia disassembly [33, 43]. We found that stimulation with Wnt3a and Wnt5a did not affect cilia assembly or disassembly respectively in Prdx5 knockdown cells. Interestingly, stimulation with Wnt3a resulted in the activation of the canonical Wnt signaling pathway in Prdx5 knockdown cells as indicated by the increased expression of Axin2 and active β-Catenin. However, the expression of non-canonical Wnt signaling target gene Ptk7 did not change when stimulated Wnt5a ligand. In this context, it is safe to speculate that the observed inhibition of ciliogenesis and Wnt signaling pathways in Prdx5 knockdown cells are independent of each other.

The role of β-catenin/WNT signaling in ADPKD is controversial. Some studies report that upregulation of β-catenin/WNT target genes such as Axin2 [61], a tumor suppressor which limits and fine-tunes the pathway [62] enhance cyst growth. Other studies however failed to detect β-catenin/TCF reporter activation in several PKD murine models [63]. This raises the question of whether β-catenin signaling is universally activated in PKD. To add to the complexity of this pathway, some studies suggest that loss of function of β-catenin promotes cyst growth [64]. In this study, we found that knockdown of Prdx5 resulted in the downregulation of multiple canonical and non-canonical Wnt ligands and target genes, indicating the inhibition of the canonical β-catenin/WNT and the PCP/non-canonical Wnt signaling pathways. However, given the multiple processes involved in Wnt signaling, the specific pathway activated by a Wnt ligand is more complex and context dependent. Our data reinforces a more complex role for Wnt signaling in ADPKD disease progression and should be taken in account when designing potential therapeutic strategies that utilize Wnt-targeting drugs to delay disease progression.

In ADPKD, cyst expansion is accompanied by renal fibrosis leading to end-stage renal failure. Prdx5 has been reported to play a protective role in the pathophysiology of renal fibrosis in unilateral ureteral obstruction (UUO) rats and renal interstitial fibroblasts [65]. We found that knockdown of Prdx5, as confirmed with Western blot and qRT-PCR analysis (Supplemental Figure 8A), increased the mRNA levels of fibrotic markers, including alpha-smooth muscle actin (α-Sma) and type I collagen (Col1), in NIH3T3 cells compared to those in control cells (Supplemental Figure 8B and 8C). We further found that knockdown of Prdx5 resulted in the increase of mRNAs of α-Sma, Col1 and fibronectin (FN) in *Pkd1* homozygous PN24 cells (Supplemental Figure 8D – 8F). These results suggest that the

downregulation of Prdx5 may also be associated with the pathophysiology of renal fibrosis in ADPKD.

It is important to highlight the limitations of this study. First, we only examined whether loss of Prdx5 promoted cyst growth in 3D cultures *in vitro*. Second, we could not test whether induction of Prdx5 delays cyst growth *in vivo* since the inducer and the activator of PRDX5 is not available. During the testing of the pharmacological effect of inhibiting Plk1, we observed that the expression of Prdx5 could be upregulated. Therefore, the combination of an effective Prdx5 inducer when it is available with Plk1 inhibitor and other ADPKD treatment drugs may be a potential therapeutic strategy and is worthy of further exploration.

Collectively, we show that knockdown of Prdx5 may be sufficient to induce cystogenesis, independent of PKD gene mutations. The cystic phenotype is likely caused by a combination of factors including: (a) induction of oxidative stress which disrupts cell cycle and cell proliferation, (b) defects in centrosome duplication and cytokinesis which result in genomic instability, (c) ciliogenesis defects that persist with the expression of Plk1, and (d) dysregulation of the canonical and non-canonical Wnt signaling pathways; all of which are reported to contribute to ADPKD disease progression. Particularly, we identify a novel Prdx5-Plk1 axis in the regulation of ciliogenesis and cyst growth, in addition to other identified mechanisms associated with Prdx5 in these processes. As such, extrapolating our results to studies performed in murine PKD models, where activation of antioxidants is suggested to improve cyst growth and renal function, we speculate that activation of Prdx5 could serve as a potential therapeutic target for the treatment of ADPKD.

Supplementary Material

Refer to Web version on PubMed Central for supplementary material.

Acknowledgements

Funding: X. Li acknowledges support from National Institutes of Health grant R01 DK129241 and DK126662 and from the PKD Foundation. J.P. Calvet acknowledges support from the PKD Foundation and from the Kansas Research and Translation Core Center (U54DK126126).

Abbreviations

Ac α tub	Acetylated-α-tubulin
ADPKD	Autosomal dominant polycystic kidney disease
AURA	Aurora kinase A
AXIN2	Axin-related protein 2
BUN	Blood urea nitrogen
Col 1	Collagen type 1
DBA	Dolichos biflorus agglutinin
FN	Fibronectin

H_2O_2	Hydrogen peroxide
4-HNE	4-hydroxynonenal
HO-1	Heme oxygenase-1
IMCD	Inner medullar collecting duct
KW/BW	Kidney weight to body weight ratio
LTL	Lotus tetragonolobus lectin
MEK	Mouse embryonic kidney
NHK	Normal human kidney
PC1	Polycystin-1
PC2	Polycystin-2
PCP	Planar cell polarity
PH2	Pkd1 heterozygous
p H3	Phospho histone H3
PKD	Polycystic kidney disease
PLK1	Polo-like kinase 1
PN24	Pkd1 null
PRDX5	Peroxiredoxin 5
Ptk7	Protein tyrosine kinase 7
qRT-PCR	Quantitative real-time polymerase chain reaction
ROS	Reactive oxygen species
RPE	Retinal pigment epithelial
TNF-α	Tumor necrosis factor-alpha
α-SMA	Alpha-smooth muscle actin

References

1. Ma M, Gallagher AR, and Somlo S, Ciliary Mechanisms of Cyst Formation in Polycystic Kidney Disease. Cold Spring Harbor Perspectives in Biology, 2017. 9(11).
2. Mochizuki T, et al. , PKD2, a gene for polycystic kidney disease that encodes an integral membrane protein. Science, 1996. 272(5266): p. 1339–1342. [PubMed: 8650545]
3. Polycystic kidney disease: the complete structure of the PKD1 gene and its protein. The International Polycystic Kidney Disease Consortium. Cell, 1995. 81(2): p. 289–98. [PubMed: 7736581]

4. Gerdes JM, Davis EE, and Katsanis N, The Vertebrate Primary Cilium in Development, Homeostasis, and Disease. Cell, 2009. 137(1): p. 32–45. [PubMed: 19345185]
5. Hildebrandt F, Benzing T, and Katsanis N, Ciliopathies. N Engl J Med, 2011. 364(16): p. 1533–43. [PubMed: 21506742]
6. Nigg EA and Raff JW, Centrioles, centrosomes, and cilia in health and disease. Cell, 2009. 139(4): p. 663–78. [PubMed: 19914163]
7. Hockenbery DM, et al. , Bcl-2 functions in an antioxidant pathway to prevent apoptosis. Cell, 1993. 75(2): p. 241–51. [PubMed: 7503812]
8. Veis DJ, et al. , Bcl-2-deficient mice demonstrate fulminant lymphoid apoptosis, polycystic kidneys, and hypopigmented hair. Cell, 1993. 75(2): p. 229–40. [PubMed: 8402909]
9. Sies H, Berndt C, and Jones DP, Oxidative Stress. Annu Rev Biochem, 2017. 86: p. 715–748. [PubMed: 28441057]
10. Poprac P, et al. , Targeting Free Radicals in Oxidative Stress-Related Human Diseases. Trends Pharmacol Sci, 2017. 38(7): p. 592–607. [PubMed: 28551354]
11. Maser RL, et al. , Oxidant stress and reduced antioxidant enzyme protection in polycystic kidney disease. J Am Soc Nephrol, 2002. 13(4): p. 991–999. [PubMed: 11912258]
12. Knoops B, et al. , Peroxiredoxin 5: Structure, Mechanism, and Function of the Mammalian Atypical 2-Cys Peroxiredoxin. Antioxidants & Redox Signaling, 2011. 15(3): p. 817–829. [PubMed: 20977338]
13. Seo MS, et al. , Identification of a new type of mammalian peroxiredoxin that forms an intramolecular disulfide as a reaction intermediate. Journal of Biological Chemistry, 2000. 275(27): p. 20346–20354.
14. Plaisant F, et al. , Recombinant peroxiredoxin 5 protects against excitotoxic brain lesions in newborn mice. Free Radical Biology and Medicine, 2003. 34(7): p. 862–872. [PubMed: 12654475]
15. Kropotov A, et al. , Mitochondrial targeting of human peroxiredoxin V protein and regulation of PRDX5 gene expression by nuclear transcription factors controlling biogenesis of mitochondria. Febs Journal, 2007. 274(22): p. 5804–5814.
16. Karihtala P, et al. , Peroxiredoxins in breast carcinoma. Clinical Cancer Research, 2003. 9(9): p. 3418–3424. [PubMed: 12960131]
17. Gerard AC, et al. , Peroxiredoxin 5 expression in the human thyroid gland. Thyroid, 2005. 15(3): p. 205–9. [PubMed: 15785239]
18. Bur H, et al. , Oxidative stress markers and mitochondrial antioxidant enzyme expression are increased in aggressive Hodgkin lymphomas. Histopathology, 2014. 65(3): p. 319–327. [PubMed: 24698430]
19. Wang MX, et al. , Expression and regulation of peroxiredoxin 5 in human osteoarthritis. FEBS Lett, 2002. 531(2): p. 359–62. [PubMed: 12417342]
20. Ma Y, et al. , Knockdown of peroxiredoxin 5 inhibits the growth of osteoarthritic chondrocytes via upregulating Wnt/beta-catenin signaling. Free Radic Biol Med, 2014. 76: p. 251–60. [PubMed: 25236745]
21. Fernandez-Ranvier GG, et al. , Candidate diagnostic markers and tumor suppressor genes for adrenocortical carcinoma by expression profile of genes on chromosome 11q13. World Journal of Surgery, 2008. 32(5): p. 873–881. [PubMed: 18324346]
22. Nauli SM, et al. , Polycystins 1 and 2 mediate mechanosensation in the primary cilium of kidney cells. Nature Genetics, 2003. 33(2): p. 129–137. [PubMed: 12514735]
23. Li XG, et al. , Polycystin-1 and polycystin-2 regulate the cell cycle through the helix-loop-helix inhibitor ld2. Nature Cell Biology, 2005. 7(12): p. 1202–1212. [PubMed: 16311606]
24. Shibazaki S, et al. , Cyst formation and activation of the extracellular regulated kinase pathway after kidney specific inactivation of Pkd1. Hum Mol Genet, 2008. 17(11): p. 1505–16. [PubMed: 18263604]
25. Drummen GPC, et al. , C11-BODIPY581/591, an oxidation-sensitive fluorescent lipid peroxidation probe: (Micro)spectroscopic characterization and validation of methodology. Free Radical Biology and Medicine, 2002. 33(4): p. 473–490. [PubMed: 12160930]

26. Ling NXY, et al. , mTORC1 directly inhibits AMPK to promote cell proliferation under nutrient stress. Nature Metabolism, 2020. 2(1): p. 41–+.
27. Mayer C and Grummt I, Ribosome biogenesis and cell growth: mTOR coordinates transcription by all three classes of nuclear RNA polymerases. Oncogene, 2006. 25(48): p. 6384–6391. [PubMed: 17041624]
28. Fujita H, Yoshino Y, and Chiba N, Regulation of the centrosome cycle. Molecular & Cellular Oncology, 2016. 3(2).
29. Loncarek J, Hergert P, and Khodjakov A, Centriole reduplication during prolonged interphase requires procentriole maturation governed by Plk1. Curr Biol, 2010. 20(14): p. 1277–82. [PubMed: 20656208]
30. Goepfert TM, et al. , Centrosome amplification and overexpression of aurora A are early events in rat mammary carcinogenesis. Cancer Res, 2002. 62(14): p. 4115–22. [PubMed: 12124350]
31. Lin F, et al. , Kidney-specific inactivation of the KIF3A subunit of kinesin-II inhibits renal ciliogenesis and produces polycystic kidney disease. Proc Natl Acad Sci U S A, 2003. 100(9): p. 5286–91. [PubMed: 12672950]
32. Pazour GJ, et al. , Chlamydomonas IFT88 and its mouse homologue, polycystic kidney disease gene tg737, are required for assembly of cilia and flagella. J Cell Biol, 2000. 151(3): p. 709–18. [PubMed: 11062270]
33. Lee KH, et al. , Identification of a novel Wnt5a-CK1varepsilon-Dvl2-Plk1-mediated primary cilia disassembly pathway. EMBO J, 2012. 31(14): p. 3104–17. [PubMed: 22609948]
34. Wang G, et al. , PCM1 recruits Plk1 to the pericentriolar matrix to promote primary cilia disassembly before mitotic entry. Journal of Cell Science, 2013. 126(6): p. 1355–1365. [PubMed: 23345402]
35. Gjertsen BT and Schoffski P, Discovery and development of the Polo-like kinase inhibitor volasertib in cancer therapy. Leukemia, 2015. 29(1): p. 11–19. [PubMed: 25027517]
36. Yoder BK, Hou X, and Guay-Woodford LM, The polycystic kidney disease proteins, polycystin-1, polycystin-2, polaris, and cystin, are co-localized in renal cilia. J Am Soc Nephrol, 2002. 13(10): p. 2508–16. [PubMed: 12239239]
37. Seeger-Nukpezah T, et al. , The Centrosomal Kinase Plk1 Localizes to the Transition Zone of Primary Cilia and Induces Phosphorylation of Nephrocystin-1. Plos One, 2012. 7(6).
38. Li A, et al. , Canonical Wnt inhibitors ameliorate cystogenesis in a mouse ortholog of human ADPKD. JCI Insight, 2018. 3(5).
39. Lee EJ, et al. , TAZ/Wnt-beta-catenin/c-MYC axis regulates cystogenesis in polycystic kidney disease. Proc Natl Acad Sci U S A, 2020. 117(46): p. 29001–29012. [PubMed: 33122431]
40. Lancaster MA, et al. , Impaired Wnt-beta-catenin signaling disrupts adult renal homeostasis and leads to cystic kidney ciliopathy. Nature Medicine, 2009. 15(9): p. 1046–U101.
41. Lee KH, Involvement of Wnt signaling in primary cilia assembly and disassembly. FEBS J, 2020. 287(23): p. 5027–5038. [PubMed: 33015954]
42. Wuebken A and Schmidt-Ott KM, WNT/beta-catenin signaling in polycystic kidney disease. Kidney International, 2011. 80(2): p. 135–139. [PubMed: 21720305]
43. Kyun ML, et al. , Wnt3a Stimulation Promotes Primary Ciliogenesis through beta-Catenin Phosphorylation-Induced Reorganization of Centriolar Satellites. Cell Reports, 2020. 30(5): p. 1447–+. [PubMed: 32023461]
44. Torres VE, et al. , Aggravation of polycystic kidney disease in Han:SPRD rats by buthionine sulfoximine. J Am Soc Nephrol, 1997. 8(8): p. 1283–91. [PubMed: 9259355]
45. Lu Y, et al. , Activation of NRF2 ameliorates oxidative stress and cystogenesis in autosomal dominant polycystic kidney disease. Sci Transl Med, 2020. 12(554).
46. Battini L, et al. , Loss of polycystin-1 causes centrosome amplification and genomic instability. Hum Mol Genet, 2008. 17(18): p. 2819–33. [PubMed: 18566106]
47. Kim MH, et al. , Peroxiredoxin 5 ameliorates obesity-induced non-alcoholic fatty liver disease through the regulation of oxidative stress and AMP-activated protein kinase signaling. Redox Biology, 2020. 28.

48. Argyropoulou V, et al. , Peroxiredoxin-5 as a Novel Actor in Inflammation and Tumor Suppression. Free Radical Biology and Medicine, 2016. 100: p. S92–S92.

49. Rezatabar S, et al. , RAS/MAPK signaling functions in oxidative stress, DNA damage response and cancer progression. Journal of Cellular Physiology, 2019. 234(9): p. 14951–14965.

50. Lin XR, et al. , The role of Aurora-A in human cancers and future therapeutics. American Journal of Cancer Research, 2020. 10(9): p. 2705–2729. [PubMed: 33042612]

51. Su LJ, et al. , Reactive Oxygen Species-Induced Lipid Peroxidation in Apoptosis, Autophagy, and Ferroptosis. Oxidative Medicine and Cellular Longevity, 2019. 2019.

52. Menezes LF, et al. , Fatty Acid Oxidation is Impaired in An Orthologous Mouse Model of Autosomal Dominant Polycystic Kidney Disease. Ebiomedicine, 2016. 5: p. 183–192. [PubMed: 27077126]

53. Zhang X, et al. , Ferroptosis Promotes Cyst Growth in Autosomal Dominant Polycystic Kidney Disease Mouse Models. J Am Soc Nephrol, 2021. 32(11): p. 2759–2776. [PubMed: 34716241]

54. Ma M, et al. , Loss of cilia suppresses cyst growth in genetic models of autosomal dominant polycystic kidney disease. Nat Genet, 2013. 45(9): p. 1004–12. [PubMed: 23892607]

55. Liu Z, Sun Q, and Wang X, PLK1, A Potential Target for Cancer Therapy. Transl Oncol, 2017. 10(1): p. 22–32. [PubMed: 27888710]

56. Tyagi S, et al. , Polo-like kinase1 (Plk1) knockdown enhances cisplatin chemosensitivity via up-regulation of p73alpha in p53 mutant human epidermoid squamous carcinoma cells. Biochem Pharmacol, 2010. 80(9): p. 1326–34. [PubMed: 20655883]

57. Gleixner KV, et al. , Polo-like Kinase 1 (Plk1) as a Novel Drug Target in Chronic Myeloid Leukemia: Overriding Imatinib Resistance with the Plk1 Inhibitor BI 2536. Cancer Research, 2010. 70(4): p. 1513–1523. [PubMed: 20145140]

58. Kim JI, et al. , Reduction of oxidative stress during recovery accelerates normalization of primary cilia length that is altered after ischemic injury in murine kidneys. Am J Physiol Renal Physiol, 2013. 304(10): p. F1283–94. [PubMed: 23515720]

59. Graves JA, et al. , Regulation of Reactive Oxygen Species Homeostasis by Peroxiredoxins and c-Myc. Journal of Biological Chemistry, 2009. 284(10): p. 6520–6529.

60. Zhou X, et al. , Therapeutic targeting of BET bromodomain protein, Brd4, delays cyst growth in ADPKD. Human Molecular Genetics, 2015. 24(14): p. 3982–3993. [PubMed: 25877301]

61. Lal M, et al. , Polycystin-1 C-terminal tail associates with beta-catenin and inhibits canonical Wnt signaling. Hum Mol Genet, 2008. 17(20): p. 3105–17. [PubMed: 18632682]

62. Bernkopf DB, et al. , An aggregon in conductin/axin2 regulates Wnt/beta-catenin signaling and holds potential for cancer therapy. Nat Commun, 2019. 10(1): p. 4251. [PubMed: 31534175]

63. Miller MM, et al. , T-cell factor/beta-catenin activity is suppressed in two different models of autosomal dominant polycystic kidney disease. Kidney International, 2011. 80(2): p. 147–154.

64. Zhou D, et al. , Tubule-specific ablation of endogenous beta-catenin aggravates acute kidney injury in mice. Kidney Int, 2012. 82(5): p. 537–47. [PubMed: 22622501]

65. Choi HI, et al. , Peroxiredoxin 5 Protects TGF-beta Induced Fibrosis by Inhibiting Stat3 Activation in Rat Kidney Interstitial Fibroblast Cells. PLoS One, 2016. 11(2): p. e0149266. [PubMed: 26872211]

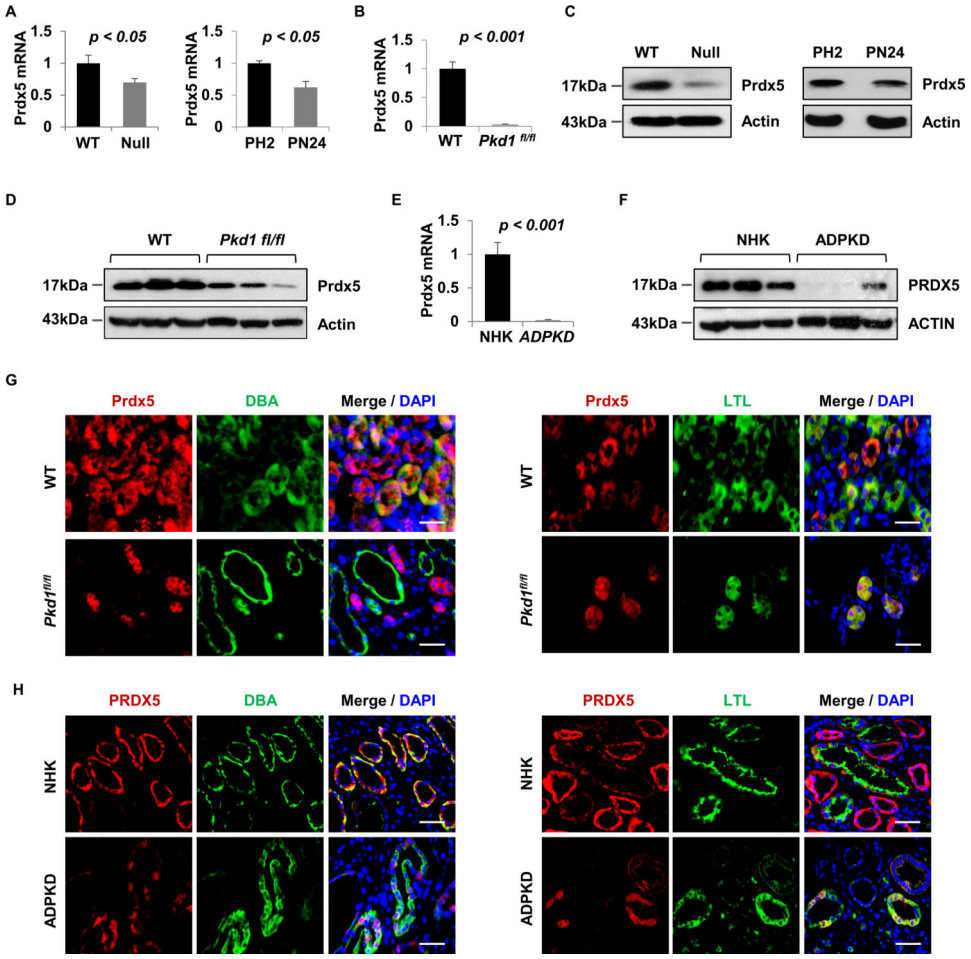

Figure 1. The expression of Prdx5 is decreased in *Pkd1* mutant renal epithelial cells and tissues.

(**A** and **B**) The expression of Prdx5 in Pkd1 (WT) and Pkd1 mutant (Null) MEK cells, and in postnatal Pkd1 heterozygous (PH2) cells and Pkd1 homozygous (PN24) cells was examined by qRT-PCR (**A**) and Western blot (**B**) analysis. (**C** and **E**) The expression of Prdx5 in postnatal day 21 kidneys from *Pkd1*$^{+/+}$*: Pkhd1-Cre* (WT) and *Pkd1*$^{fl/fl}$*: Pkhd1-Cre* (*Pkd1*$^{fl/fl}$) mice was examined by qRT-PCR (**C**) and Western blot (**D**) analysis. (**E** and **F**) The expression of PRDX5 in kidneys from ADPKD patients and normal individuals as examined by qRT-PCR (**E**) and Western blot (**F**) analysis. (**E**) Immunofluorescent staining of Prdx5 expression co-stained with DBA or LTL, in postnatal day 21 kidney sections from *Pkd1*$^{+/+}$*: Pkhd1-Cre* (WT) and *Pkd1*$^{fl/fl}$*: Pkhd1-Cre* (*Pkd1*$^{fl/fl}$) mice (n=3). The staining indicated that Prdx5 expression was decreased in cyst-lining epithelia in *Pkd1* mutant kidneys. (**H**) Immunofluorescent analysis of PRDX5 expression co-stained with DBA or LTL, in kidneys from ADPKD patients and normal individuals (n=3). The staining indicated that Prdx5 expression was decreased in cyst-lining epithelia in ADPKD kidneys. Scale bars, 20 μm.

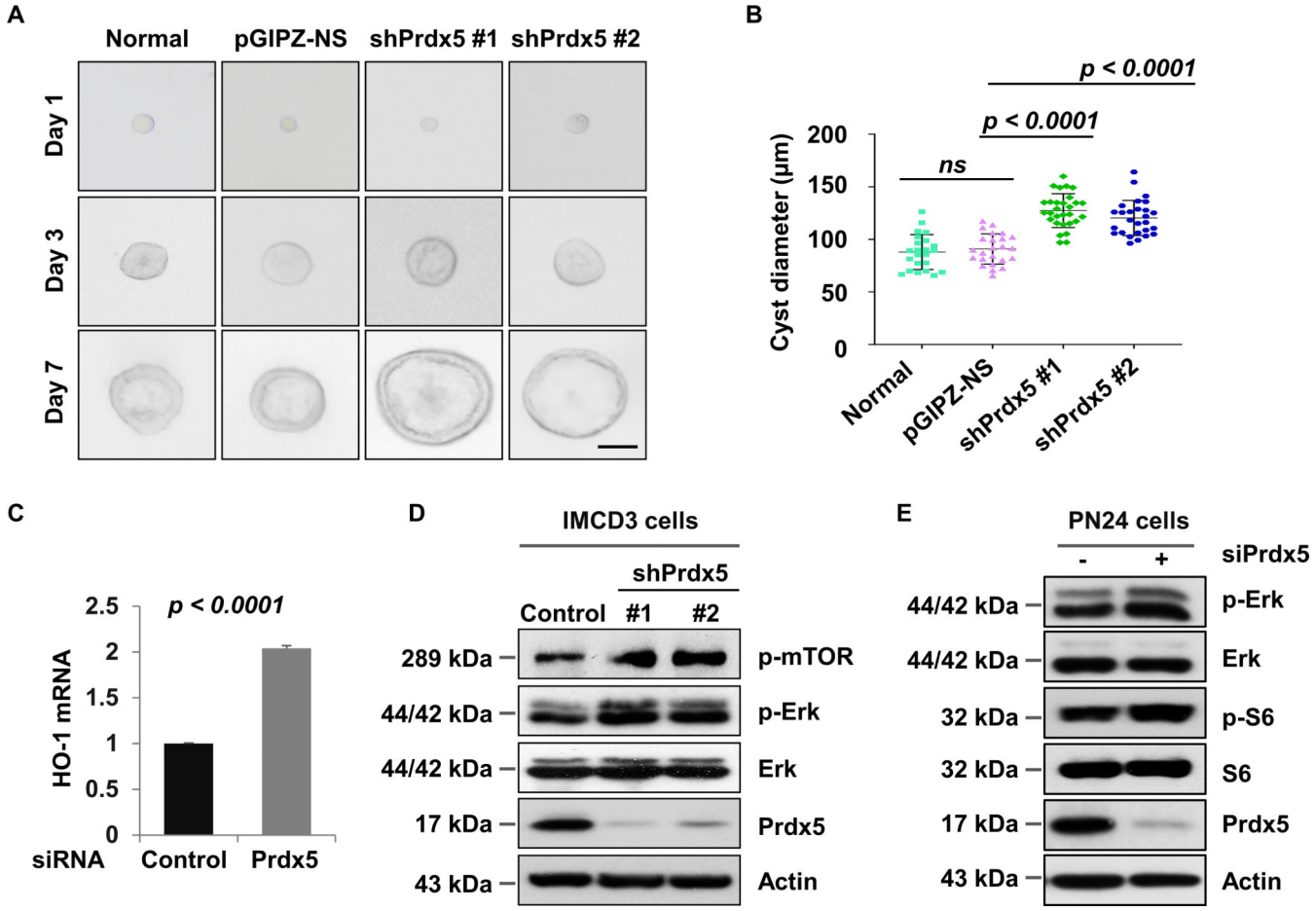

Figure 2. Knockdown of Prdx5 promotes spheroid (cyst) growth by activating mTOR and Erk pathways.

(**A**) Light micrographs of cysts formed in Matrigel with Prdx5 stable knockdown mIMCD3 cells (clone #1) at days 1, 3 and 7. Scale bars, 100 μm. (**B**) Cyst diameters of 3D cultures of Prdx5 stable knockdown mIMCD3 cells (clone #1) on day 7. A minimum of 25 spheroids for each group from three different experiments were evaluated. Error bars represent the SD. (**C**) The expression of HO-1 in *Pkd1* homozygous PN24 cells transfected with Prdx5 or control siRNA examined by qRT-PCR analysis. (**D**) The expression of the phosphorylation of mTOR1 and Erk, as well as the total protein level of Erk was examined by Western blot in Prdx5 stable knockdown mIMCD3 cells. (**E**) Western blot analysis of the expression of the phosphorylation of Erk and S6, as well as the total levels of these proteins in *Pkd1* homozygous PN24 transfected with Prdx5 siRNA or control siRNA for 48 h.

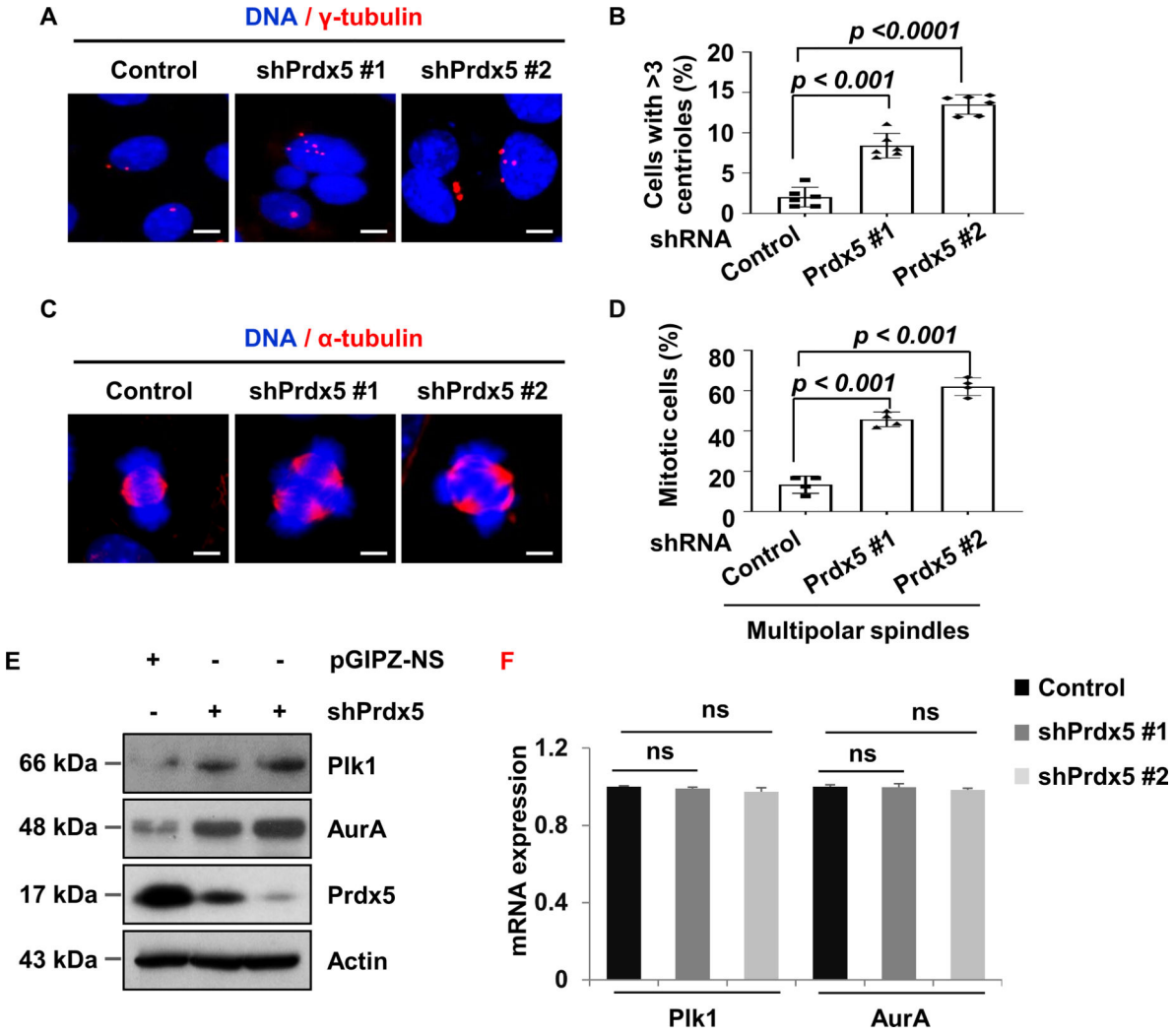

Figure 3. Prdx5 regulates centrosome amplification and spindle integrity.

(**A**) Knockdown of Prdx5 increased centrosome amplification in mouse IMCD3 cells compared to control cells stained with γ-tubulin (red) and DAPI and visualized by fluorescence microscopy. Scale bars, 5 μm. (**B**) Quantification analysis of the percentage of cells exhibiting abnormal centrosome amplification (cells with ≥3 centrosomes). Error bars represent the SD. (**C**) Knockdown of Prdx5 induced the formation of multipolar spindles stained with α-tubulin (red) and DAPI. Scale bars, 5 μm. (**D**) Quantification analysis of the percentage of mitotic cells with multipolar spindles in Prdx5 stable knockdown mouse IMCD3 cells compared to control cells. Error bars represent the SD. (**E**) Western blot analysis of the levels of the Plk1 and AurA in Prdx5 stable knockdown mIMCD3 cells. (**F**) qRT-PCR analysis of relative Plk1 and AurA mRNA expression from three independent experiments in Prdx5-shRNA stable knockdown or NC-shRNA in mouse IMCD3 cells. Error bars represent the SD.

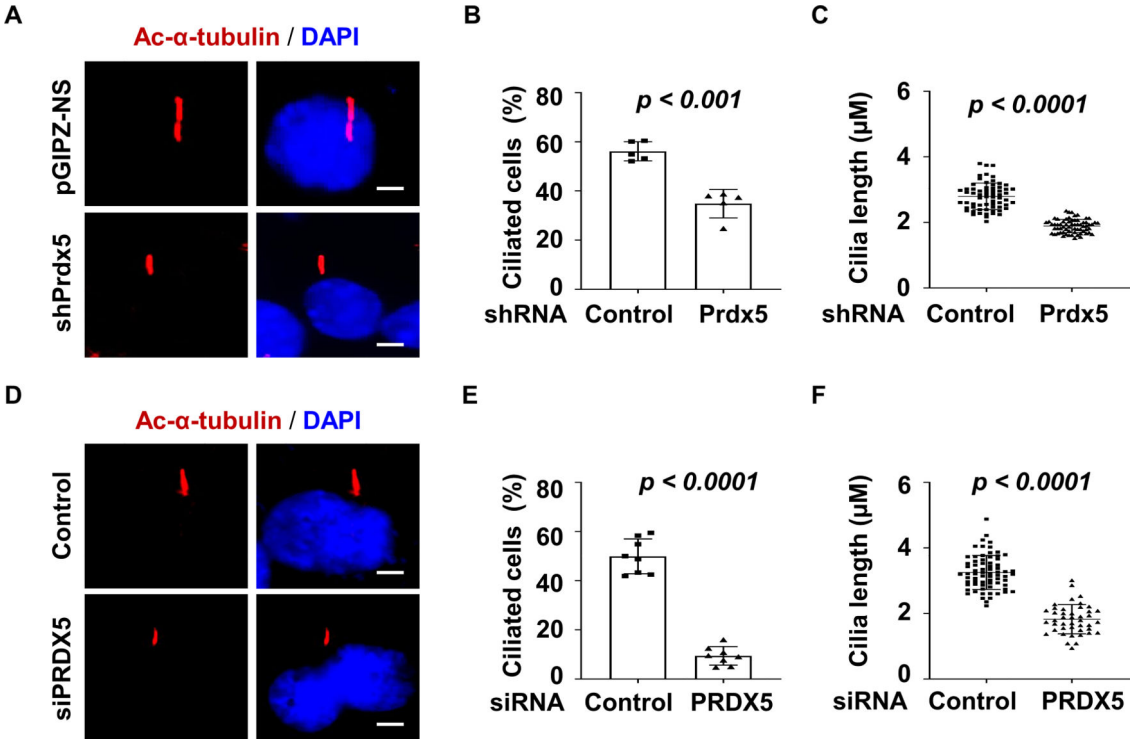

Figure 4. Depletion of Prdx5 abrogates ciliogenesis.

(**A – C)** Immunofluorescence images (**A**), percentage of ciliated cells (**B**) and ciliary length (**C**) in Prdx5 stable knockdown mouse IMCD3 cells, serum-starved for 48 h and stained with acetylated α-tubulin antibody and DAPI. Scale bar, 5 μm. Error bars represent the SD. (**D – F)** Immunofluorescence images (**D**), percentage of ciliated cells (**E**) and ciliary length (**F**) in human RPE1 cells transfected with control siRNA or PRDX5 siRNA, serum-starved for 24 h and stained with acetylated α-tubulin antibody and DAPI. Scale bars, 5 μm. Error bars represent the SD.

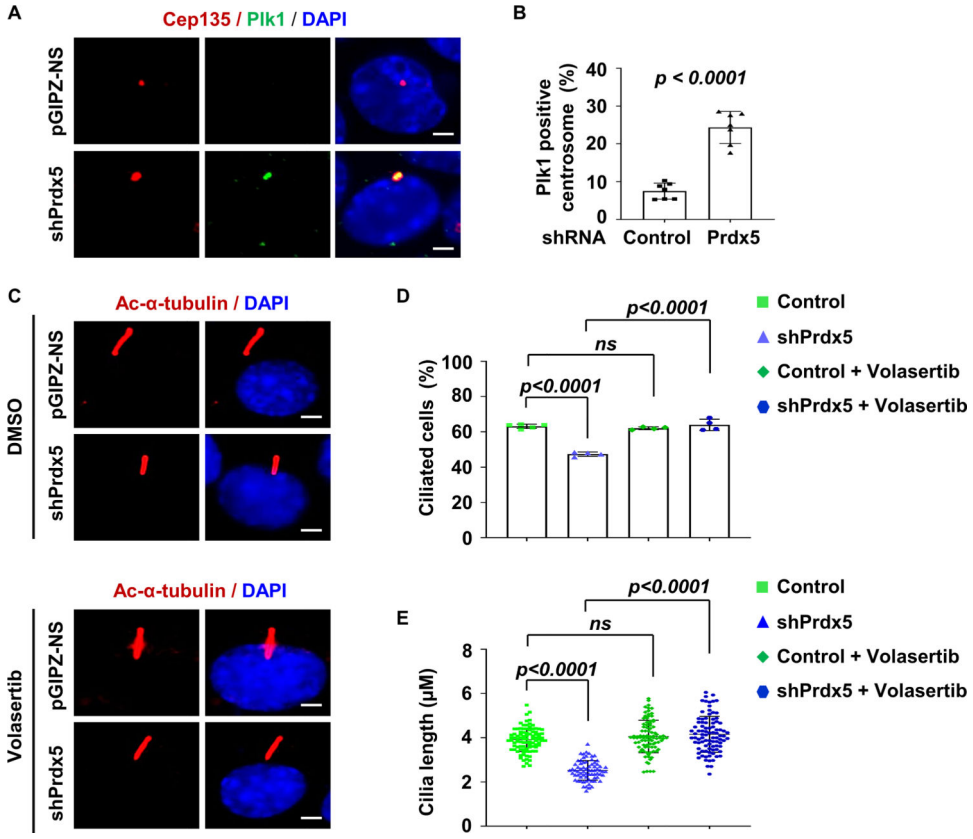

Figure 5. Inhibition of Plk1 rescues ciliogenesis in Prdx5 knockdown cells.

(**A** and **B**) Knockdown of Prdx5 increased the localization of Plk1 at the centrioles. The representative image (**A**) show that endogenous Plk1 (green), is located at the centriole in Prdx5 knockdown mouse IMCD3 cells co-stained with centriole marker Cep135 (red) and DAPI. Scale bars, 5 μm. (**B**) The quantification analysis of cells positive for Plk1 at the centriole in Prdx5 knockdown IMCD3 cells compared to control cells. Error bars represent the SD. (**C** - **E**) Inhibition of Plk1 in Prdx5 knockdown cells rescues ciliogenesis. The representative images (**C**, *top panels*) show that knockdown of Prdx5 inhibits ciliogenesis and treatment with Plk1 inhibitor volasertib (**C**, *bottom panels*) recues the ciliogenesis defect in Prdx5 knockdown IMCD3 cells. Scale bar, 5 μm. The quantification analyses of the percentage of ciliated cells (**D**), and ciliary length (**E**) in Prdx5 stable knockdown IMCD3 cells compared to control cells. Error bars represent the SD.

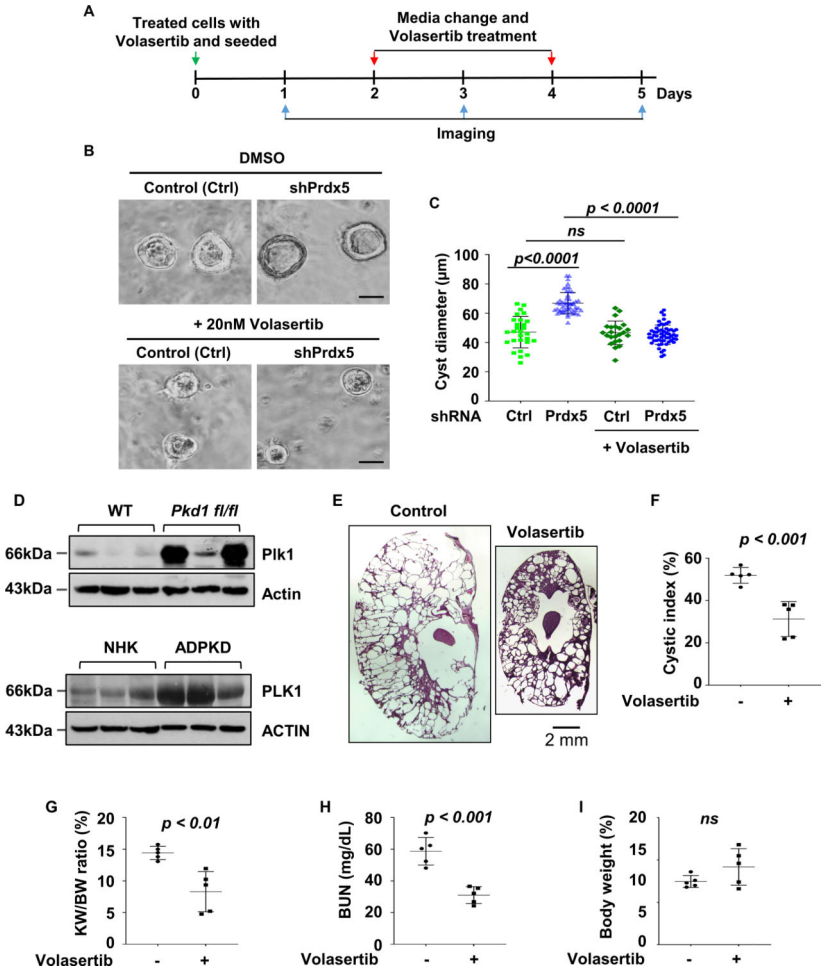

Figure 6. Inhibition of Plk1 delays cyst (spheroid) growth *in vitro* and *in vivo*.

(**A**) The experimental schedule of Plk1 inhibitor treatment and imaging times is shown. (**B**) Light micrographs of cysts formed in Matrigel on day 5. *Top panels* show control cells and Prdx5 knockdown IMCD3 cells treated with DMSO, and *bottom panels* show images for control cells and Prdx5 knockdown IMCD3 cells treated with 20nM volasertib. Scale bars, 100 μm. (**C**) Cyst diameters of 3D cultures of Prdx5 stable knockdown mIMCD3 cells treated with or without volasertib treatment on day 5. A minimum of 25 spheroids for each group from three different experiments were evaluated. Error bars represent the SD. (**D**) The expression of Plk1 in postnatal day 21 kidneys from $Pkd1^{+/+}$: Pkhd1-Cre (WT) and $Pkd1^{fl/fl}$: Pkhd1-Cre (Pkd1fl/fl) mice (*top panel*), and in human ADPKD kidneys (*bottom panel*) as examined by Western blot. (**E**) Histological examination of kidneys from *$Pkd1^{fl/fl}$:Pkhd1:Cre* mice injected daily with volasertib or DMSO vehicle control from P8 to P19. Scale bar: 2 mm. (**F**) Percent cystic area relative to total kidney area of kidneys from *$Pkd1^{fl/fl}$:Pkhd1:Cre* mice treated with volasertib (n = 5) or DMSO (n = 5). (**G** and **H**) Treatment with volasertib compared with DMSO decreased KW/BW ratios (**G**) and BUN levels (**H**) in *$Pkd1^{fl/fl}$:Pkhd1:Cre* mice. (**I**) No body weight difference was observed for the effect of volasertib on delaying cyst growth in Pkd1fl/fl: Pkhd1-Cre mice.

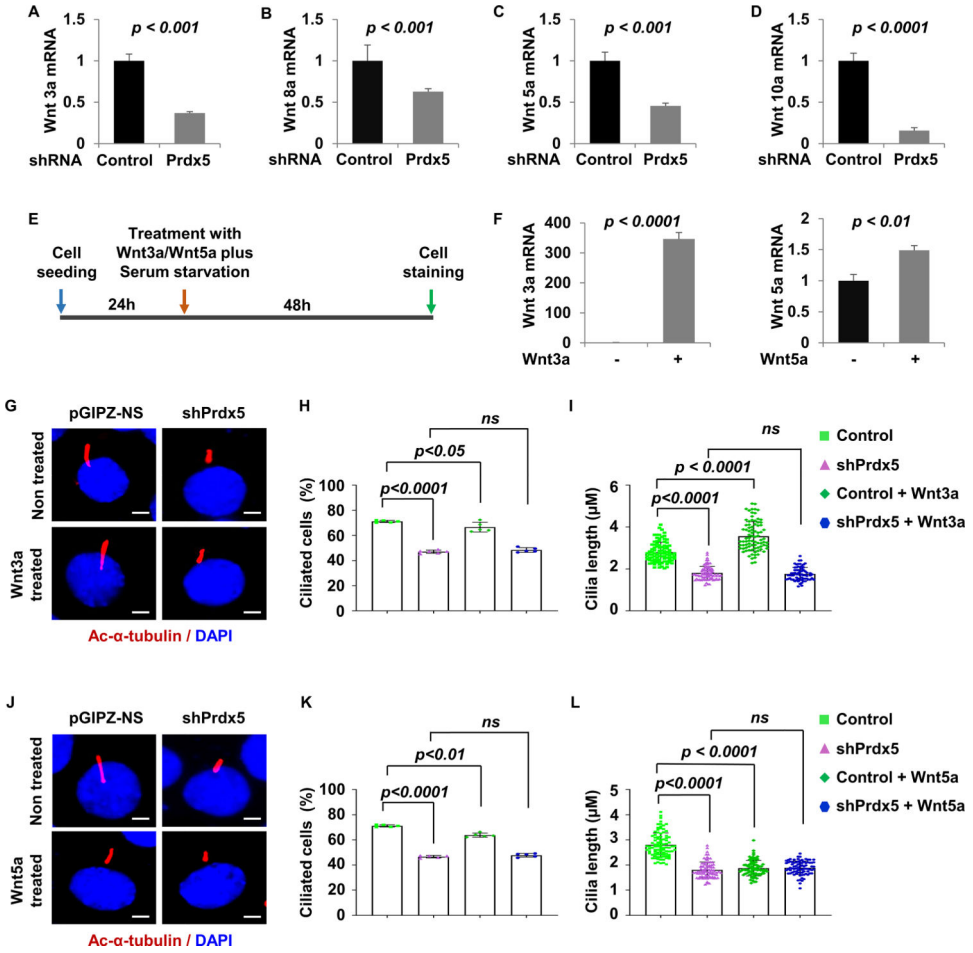

Figure 7. Knockdown of Prdx5 blocks Wnt3a and Wnt5a effect on primary ciliogenesis in IMCD3 Cells.

(**A** and **B)** The mRNA expression of canonical Wnt ligands, Wnt3a (**A**) and Wnt 8a (**B**) as examined by qRT-PCR in Prdx5 knockdown mouse IMCD3 cells compared to those in control cells. (**C** and **D**) The mRNA expression of non-canonical Wnt ligands, Wnt5a (**C**) and Wnt 10a (**D**) as examined by qRT-PCR in Prdx5 knockdown mouse IMCD3 cells compared to those in control cells. (**E** and **F**) The experimental schedule of Wnt ligand treatment (**E**), and the mRNA levels of Wnt3a and Wnt5a (**F**) upon stimulation of Wnt3a (50ng/ml) and Wnt5a (100ng/ml) respectively. The induction of Wnt3a and Wnt5a represents the positive control of Wnt3a and Wnt5a stimulation respectively. (**G – I**) The representative images (**G**) of Prdx5 knockdown and control IMCD3 cells stimulated with Wnt3a ligand with serum starvation for 48 h and immunostained with anti-acetylated α-tubulin (Ac-α-tub) and DAPI. Quantification analysis of the percentage of ciliated cells (**H**), and ciliary length (**I**), in Prdx5 stable knockdown mouse IMCD3 cells compared to control cells. Scale bar, 5 μm. (**J – L**) The representative images (**J**) of Prdx5 knockdown and control IMCD3 cells stimulated with Wnt5a ligand with serum starvation for 48 h and immunostained with anti-acetylated α-tubulin (Ac-α-tub) and DAPI. Quantification analysis of the percentage of ciliated cells (**K**), and ciliary length (**L**), in Prdx5 stable knockdown mouse IMCD3 cells compared to control cells. Scale bar, 5 μm. Error bars represent the SD.

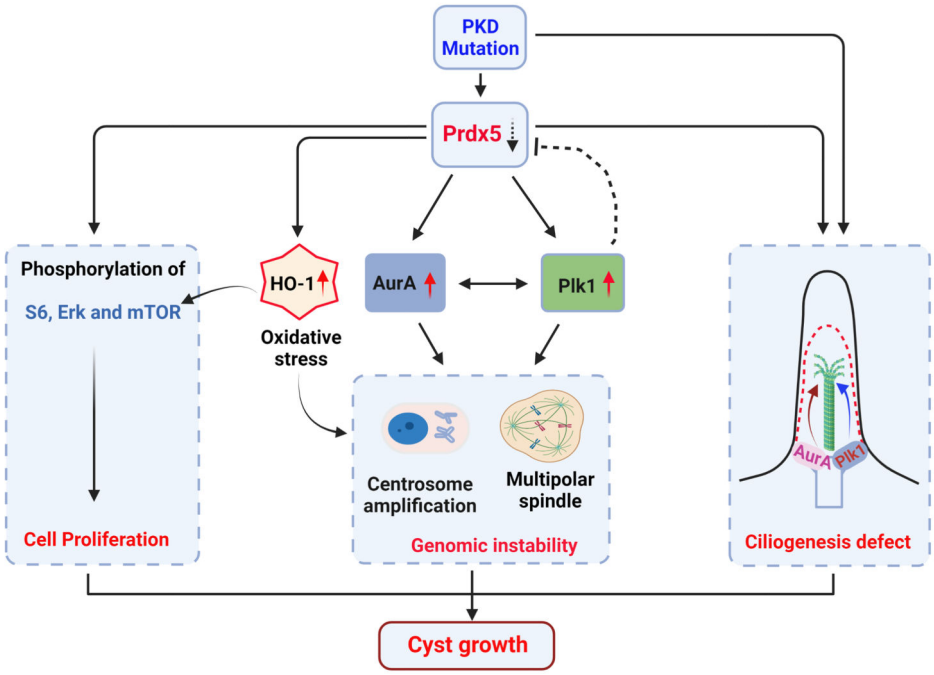

Figure 8. Working Model.

PRDX5 expression is downregulated in ADPKD. Downregulation of Prdx5 1) increases the induction of HO-1, an oxidative stress marker; 2) increases the activation of cell proliferation markers Erk, S6 and mTOR; 3) increases centrosome amplification and multipolar spindle formation which may result in genome instability reported to cause cyst growth; 4) increases the expression of Plk1 and AurA, reported to regulate cell proliferation and cell signaling; and 5) inhibits ciliogenesis, possibly by increasing the basal body localization and activity of Plk1/AurA mediated cilia disassembly; which consequently results in increased cystic renal epithelial cell proliferation in ADPKD kidneys.